DOLPHIN 4

Regularization of prestack data

A.J. Berkhout [1]
Jan Thorbecke [2]

4.1 Introduction

In CFP technology seismic processing should be applied *after* the first focusing step. In this chapter it is indicated that this also applies to regularization; it is proposed to apply regularization after focusing in detection for each hydrophone streamer (marine) or geophone spread (land).

4.2 CFP; definition and construction

The focusing process can be expressed in the $\mathbf{WRW}$ matrix formulation for up-down wave propagation. The well known DELPHI model of seismic reflection data, backscattered from one depth level at z_m, is given by

$$\mathbf{P}(z_r, z_s) = \mathbf{D}^-(z_r)\left[\mathbf{W}^-(z_r, z_m)\mathbf{R}^+(z_m)\mathbf{W}^+(z_m, z_s)\right]\mathbf{S}^+(z_s), \tag{4.1}$$

where z_r is the receiver level, z_m is the reflection level and z_s represents the source level. Focusing is defined by a weighted (in phase and amplitude) summation along the source or receiver arrays in such a way that the constructed wave front has a focus point in the subsurface. The weighting operator is also called the focusing operator. It synthesizes the response of a focusing areal source. The principle of combining shot gathers at the surface for the synthesis of areal source responses, also referred to as areal shot record technology, was already introduced

[1] E-mail: A.J.Berkhout@CTG.TUDelft.NL
[2] E-mail: J.W.Thorbecke@CTG.TUDelft.NL

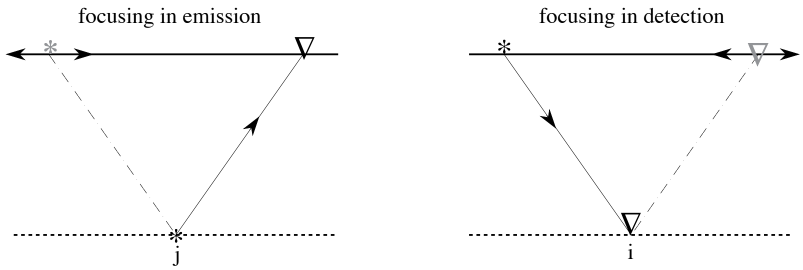

$$\vec{I}_j^+(z_m) = \mathbf{W}^+(z_m, z_0)\mathbf{S}^+(z_0)\vec{F}_j^+(z_0, z_m) \qquad \vec{F}_i^-(z_m, z_0)\mathbf{D}^-(z_0)\mathbf{W}^-(z_0, z_m) = \vec{I}_i^-(z_m)$$

$$\vec{P}_j^-(z_0, z_m) = \mathbf{W}^-(z_0, z_m)\mathbf{R}^+(z_m)\vec{I}_j^+(z_m) \qquad \vec{P}_i^-(z_m, z_0) = \vec{I}_i^-(z_m)\mathbf{R}^+(z_m)\mathbf{W}^+(z_m, z_0)\mathbf{S}^+(z_0)$$

Fig. 4.1 *Focusing in detection positions a virtual receiver on a reflecting boundary and focusing in emission positions a virtual source on a reflecting boundary.*

by Berkhout (1992) for controlled illumination in prestack depth migration. Rietveld (1995) has shown many examples for the planar areal sources.

The focusing operator for the receiver arrays, applied to the left side of the right-hand side of equation (4.1), is defined as

$$\vec{F}_i^-(z_m, z_r)\mathbf{D}^-(z_r)\mathbf{W}^-(z_r, z_m) = \vec{I}_i^-(z_m) \tag{4.2}$$

$$\vec{F}_i^-(z_m, z_r) \approx \vec{I}_i^-(z_m)\left[\mathbf{W}^+(z_m, z_r)\right]^*\left[\mathbf{D}^-(z_r)\right]^{-1} \tag{4.3}$$

with $\vec{I}_i^-(z_m)$ a unit vector with a 1 at the i^{th} position at depth z_m and $F_i^-(z_m, z_r)$ the focusing operator acting at the receiver positions at the surface (see figure 4.1). Note that the approximation in equation (4.2) refers to the approximation of the inverse of the propagation operator $\mathbf{W}^-(z_r, z_m)$ with its matched filter $\left[\mathbf{W}^-(z_r, z_m)\right]^{-1} \approx \left[\mathbf{W}^+(z_m, z_r)\right]^*$.

The focusing operator for the source arrays, applied to the right side of the right-hand side of equation (4.1), is defined as

$$\vec{I}_j^+(z_m) = \mathbf{W}^+(z_m, z_s)\mathbf{S}^+(z_s)\vec{F}_j^+(z_s, z_m) \tag{4.4}$$

$$\left[\mathbf{S}^+(z_s)\right]^{-1}\left[\mathbf{W}^-(z_s, z_m)\right]^*\vec{I}_j^+(z_m) \approx \vec{F}_j^+(z_s, z_m) \tag{4.5}$$

with $\vec{I}_j^+(z_m)$ a unit vector with a 1 at the j^{th} position at depth z_m and $\vec{F}_j^+(z_s, z_m)$ the focusing operator acting at the source positions (see figure 4.1). The focusing operators $F^\pm$ perform a summation along the receiver positions ($\vec{F}^-$) in a common shot gather or a summation along the source positions ($\vec{F}^+$) in a common receiver gather. This summation (or synthesis) is carried out for all source and receiver positions available.

Substituting equation (4.2) into equation (4.1) gives an expression of the data after focusing of the detector array

$$\vec{F}_i^-(z_m, z_r)\mathbf{P}(z_r, z_s) = \vec{P}_i^-(z_m, z_s) = \vec{I}_i^-(z_m)\mathbf{R}^+(z_m)\mathbf{W}^+(z_m, z_s)\mathbf{S}^+(z_s) \tag{4.6}$$

where equation (4.6) is an expression for the Common Focus Point (CFP) gather for detection. Substituting equation (4.4) into equation (4.1) gives an expression for the focusing of the source array

$$\mathbf{P}(z_r, z_s)\vec{F}_j^+(z_s, z_m) = \vec{P}_j(z_r, z_m) = \mathbf{D}^-(z_r)\mathbf{W}^-(z_r, z_m)\mathbf{R}^+(z_m)\vec{I}_j^+(z_m) \tag{4.7}$$

where equation (4.7) is an expression for the Common Focus Point (CFP) gather for emission.

Focusing of both the detector and the source array by combining equation (4.2) and equation (4.4) into equation (4.1) gives

$$P_{ij}^-(z_r) = \vec{F}_i^-(z_m, z_r)\mathbf{P}(z_r, z_s)\vec{F}_j^+(z_s, z_m) = \vec{I}_i^-(z_m)\mathbf{R}^+(z_m)\vec{I}_j^+(z_m) = R_{ij}^+(z_m) \tag{4.8}$$

which is the double focus result shown in figure (4.2).

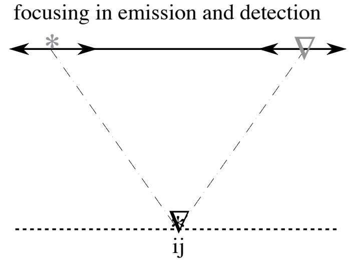

Fig. 4.2 *Focusing in detection and emission positions a virtual source and a virtual receiver on a reflecting boundary. In confocal migration i=j.*

4.3 Shot interpolation in the first focusing step

The construction of a CFP gather is explained by following the steps explained in the previous section. For this purpose numerical data, based on the model shown in figure (4.3)a, is used. The numerical data is modeled with a fixed acquisition spread where the source positions are defined at every receiver position (201 shot positions with $\Delta x = 15m$). The source has a dipole character and its signature is given by a Ricker wavelet with a frequency peak at 26.4 Hz. For the modeling an acoustic finite difference algorithm is used. The subsurface model includes a diffraction point at $z = 1000$, $x = -750$ m and a negative reflection coefficient for the wedge in the right corner of the model. Explaining the CFP processing techniques will be done with the use of this syncline model. The synthesis process for a focusing receiver with a focus point defined at the synclinal interface at $x = 0$ and $z = 950m$ (the focus point is indicated in figure (4.3a)) is shown in detail in figure (4.3).

The time reversed focusing operator $\vec{F}_i^-(z_m, z_r)$ for the defined focus point is shown in figure (4.3b). This operator is applied to all common shot gathers available. Three different common

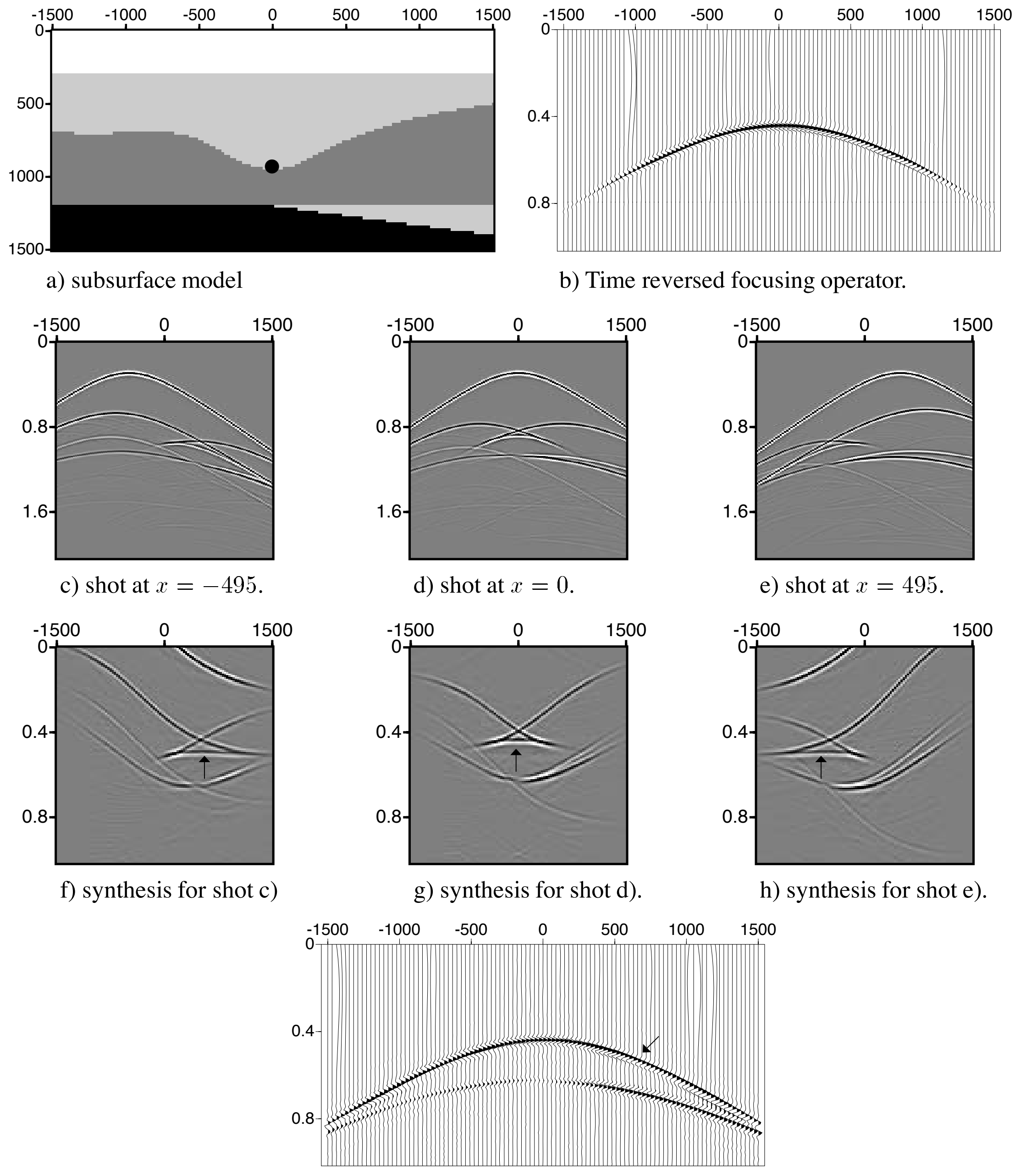

Fig. 4.3 *Synthesis of a CFP gather for focusing in detection. Every shot record contributes to one trace in the CFP gather, being positioned at the source locations. Note the contribution of the Fresnel zones in figure 4.3f,g and h. The focus point response has been indicated with an arrow (figure 4.3i). Note the relative simplicity of the CFP gather. Nota also that each event of the focus point response represents a stack within the Fresnel zone.*

shot gathers with source positions at $x = -495, z = 0$ and $x = 495$ are shown in figure (4.3) c, d and e respectively. Convolution along the time axis of the traces in the shot gathers with the traces in the focusing operator gives the intermediate synthesis results shown in figure (4.3) f, g and h. Note that in these intermediate synthesis results the bow-tie of the synclinal structure is still present. Summation over all the traces in the intermediate synthesis result gives one trace of the CFP gather. The most important contribution in the summation result is determined by the horizontally aligned traces within the Fresnel zone. The lateral position of the *centre* of the Fresnel zone is determined by following the ray-path from the source, via the focus point position, to the receiver. Thus for a 1-Dimensional medium the Fresnel zone is given by the source position mirrored in the focus point position. The time position of the Fresnel zone contribution of the event of interest is indicated by the time of the synthesis operator at the source position. If the focusing operator is correct then the time given by the operator is identical with the time in the CFP gather (for a detailed discussion see DELPHI volume VI Chapter 10). The summed trace is placed in the CFP gather at the position of the source. By carrying out the synthesis for all shot records the CFP gather for a focusing detector is constructed. In the CFP gather shown in figure 4.3i the reflection from the syncline and the deeper boundary are clearly visible. The response of the first reflector is moved outside the time window. Note that the bow-tie event in the two-way time shot gather (figure 4.3d) is focused in the CFP gather (figure 4.3i) and is therefore much simpler to interpret. In the construction of a CFP gather the shot records are transformed to a response which is less complicated.

In the first focusing step energy is focused to the selected gridpoint and the constructed CFP gather is much easier to interpret. In figure 4.4 the results on the numerical data set, based on the model in figure 4.4a, are shown. The shot record with a source position in the middle of the model is visualized in figure 4.4b. In the shot record the triplication, originating from the synclinal structure, is clearly visible. In figure 4.4c the focusing beam is shown. Note that the focusing area is not restricted to the chosen gridpoint only. Figure 4.4d illustrates that the CFP gather in much simpler than the shot record and therefore better suited for trace interpolation.

Due to the simplicity of CFP gathers, it is very advantageous to apply regularization to a CFP gather. The proposed procedure is as follows:

① **Apply focusing in detection.**
Use the fact that in practice the detectors are densely spaced along the streamers / spreads; the focusing result is a correct CFP trace at each source position.

② **Apply move-out correction.**
Use the focusing operator to remove the traveltime move-out of the CFP gather around the focus point response.

③ **Apply a regularization process.**
Use a zero-phase bandlimited spatial filter to reconstruct the samples around the focus point response at the required gridpoints.

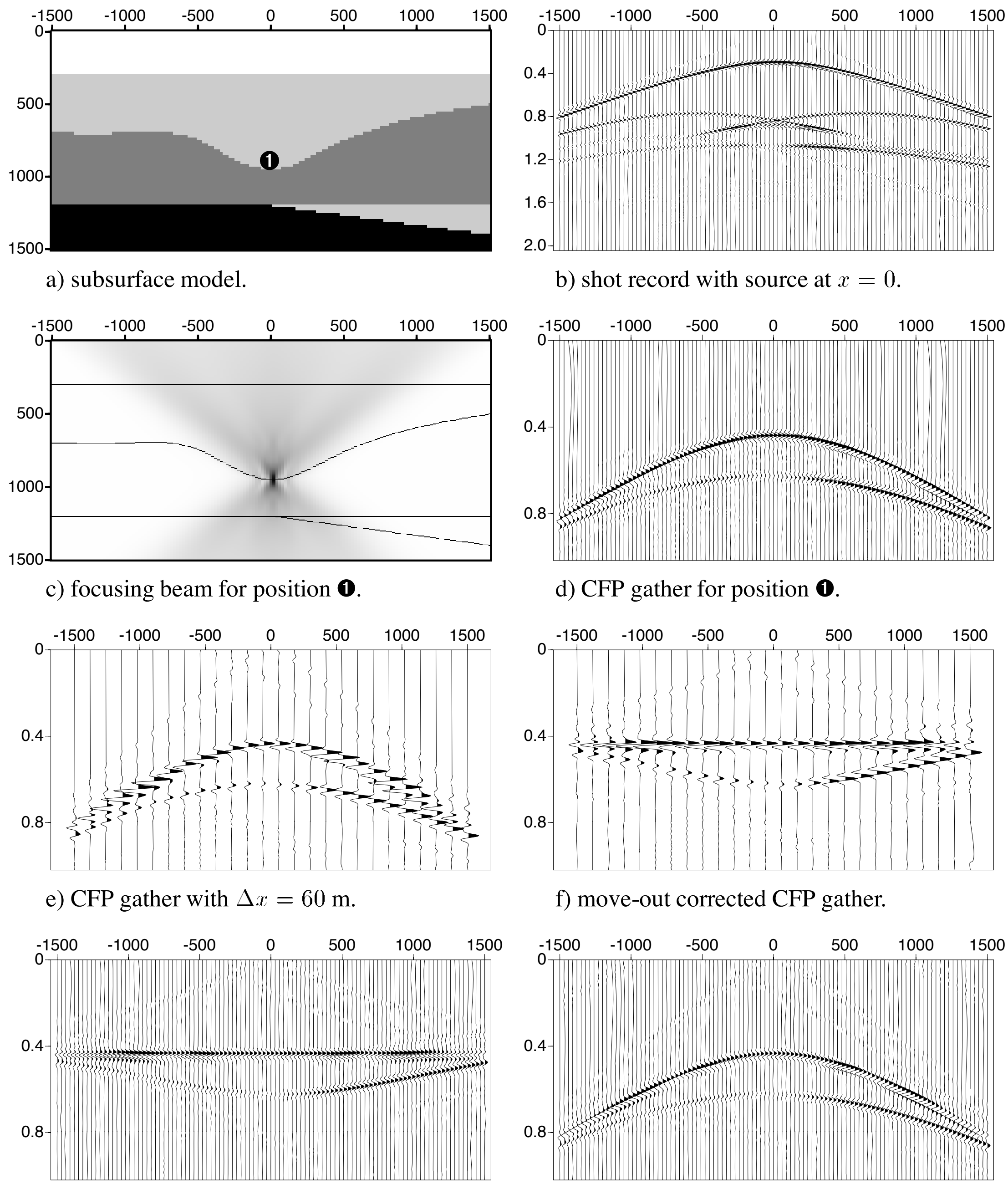

a) subsurface model.

b) shot record with source at $x = 0$.

c) focusing beam for position ❶.

d) CFP gather for position ❶.

e) CFP gather with $\Delta x = 60$ m.

f) move-out corrected CFP gather.

g) CFP gather after regridding.

h) CFP gather with $\Delta x = 15$ m.

Fig. 4.4 *CFP regularization procedure: from* 60 *m shot spacing to* 15 *m shot spacing*

After the move-out is restored again, a properly sampled CFP gather is obtained and processing can be continued.

The regularization procedure is shown in figure 4.4. We start with a CFP gather, based on focusing in detection; it is sparsely sampled in the shot positions and is shown in figure 4.4e. Removing the move-out of this CFP gather according to its operator gives the result shown in figure 4.4f. Note that the perfect alignment of the first event means that the focusing operator used to construct the CFP gather is correct. The second event, originating from the wedge in the left part of the model, is not flat but contains less move-out than the corresponding event in the CFP gather. The move-out corrected CFP gather is eminently suited for regularization due to the alignment of the event corresponding to the chosen gridpoint. The regularization can be carried out by chosing an interpolation method that can handle irregular data. In the shown examples interpolation is carried out according to the regularization algorithm described in Chapter 3. The interpolated move-out corrected CFP gather is shown in figure 4.4g. Restoring the move-out correction from the interpolated result gives the CFP gather shown in figure 4.4h. Note the excellent reconstruction.

The same interpolation procedure as shown in figure 4.4 is also used in figure 4.5 but now for a number of different shot spacings. Note that for a shot distance of 120 m the event corresponding with the chosen gridpoint can be interpolated very well, the lower event start to suffer from aliasing. This problem should be solved by applying the regularization procedure on move-out corrected multi focus CFP gathers.

Figure 4.6 show the situation with a velocity error of 20% in the first layer. Note that the regularization results are similar to the results obtained in figure 4.5.

4.4 Discussion and conclusions

It is proposed to regularize 3-D seismic data after focusing in detection for the data of each individual hydrophone streamer (marine) or geophone spread (land). For one subsurface gridpoint the focusing process yields for each streamer/spread a CFP gather with traces at the source positions. The regularization process is carried out on the operator-based move-out corrected CFP gather around the focus point response. We aim at a fast algorithm that optionally includes noise attenuation along the focus point response.

4.5 References

Berkhout, A. J., 1992, Areal shot record technology: Journal of Seismic Exploration, **1**, no. 2, 251–264.

Rietveld, W. E. A., 1995, Controlled illumination in prestack seismic migration: Ph.D. thesis, Delft University of Technology.

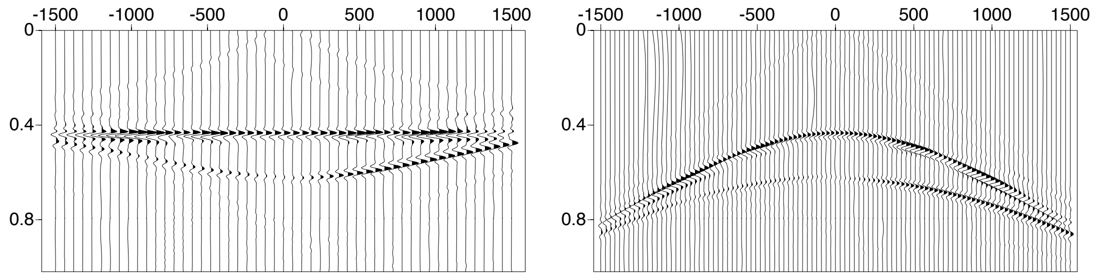

a) move-out corrected CFP gather with $\Delta x = 30$ m. b) reconstructed CFP gather with $\Delta x = 15$ m.

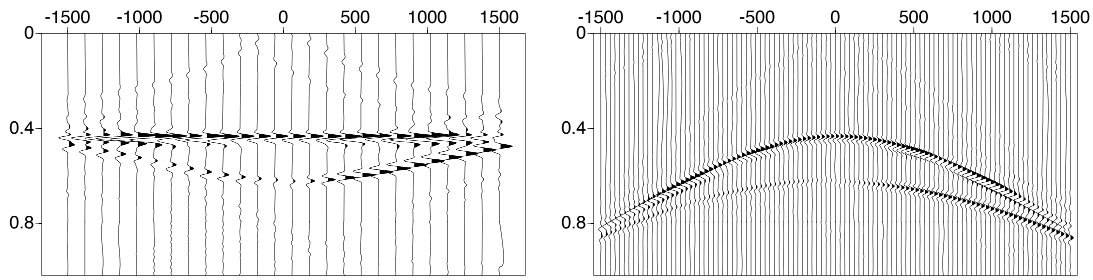

c) move-out corrected CFP gather with $\Delta x = 60$ m. d) reconstructed CFP gather with $\Delta x = 15$ m.

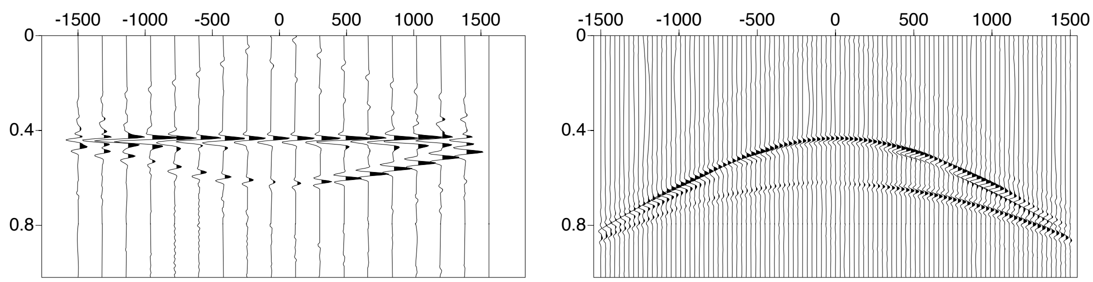

e) move-out corrected CFP gather with $\Delta x = 90$ m. f) reconstructed CFP gather with $\Delta x = 15$ m.

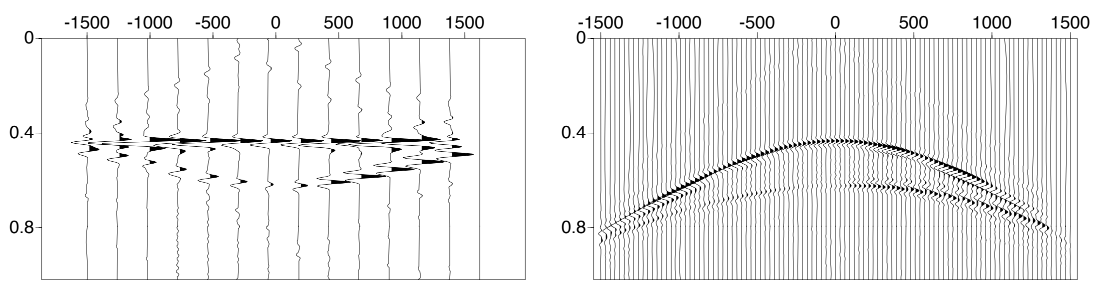

g) move-out corrected CFP gather with $\Delta x = 120$ m.h) reconstructed CFP gather with $\Delta x = 15$ m.

Fig. 4.5 *CFP regularization result.*

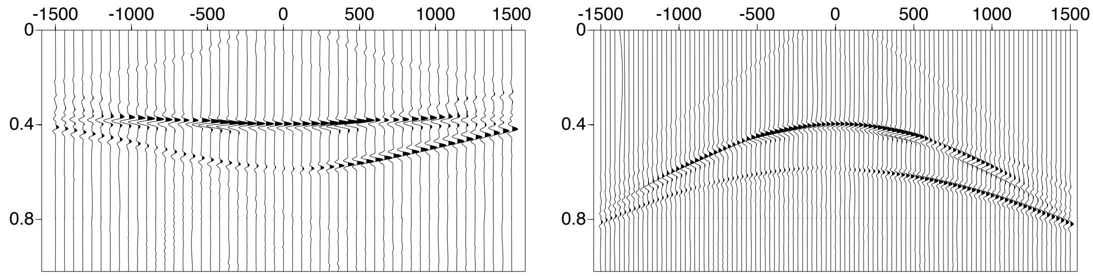

a) move-out corrected CFP gather with $\Delta x = 30$ m. b) reconstructed CFP gather with $\Delta x = 15$ m.

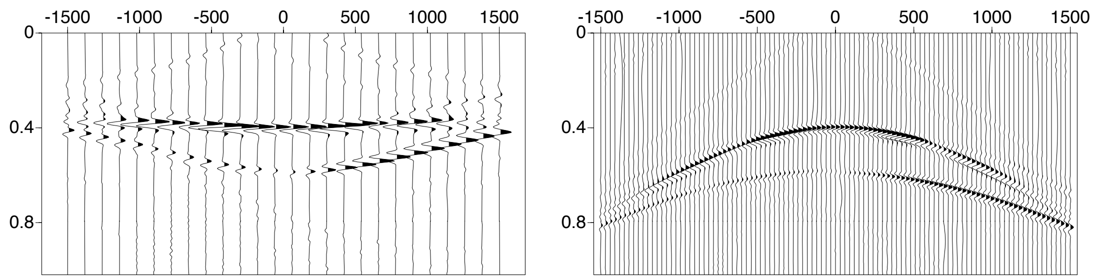

c) move-out corrected CFP gather with $\Delta x = 60$ m. d) reconstructed CFP gather with $\Delta x = 15$ m.

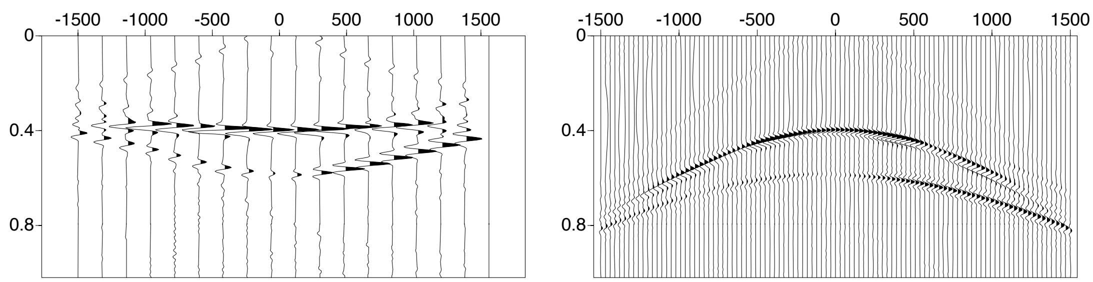

e) move-out corrected CFP gather with $\Delta x = 90$ m. f) reconstructed CFP gather with $\Delta x = 15$ m.

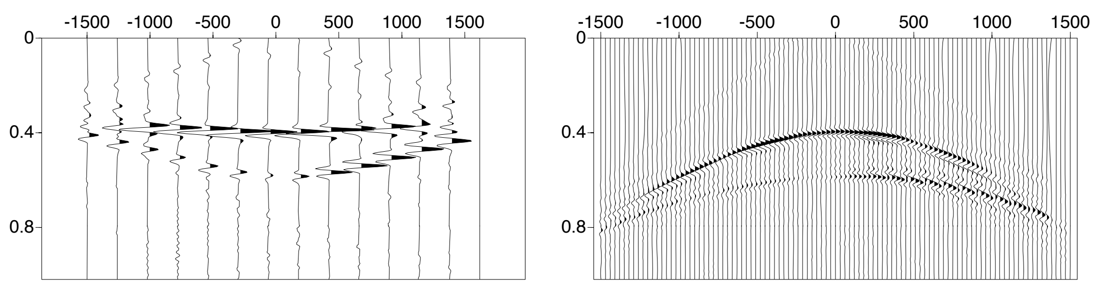

g) move-out corrected CFP gather with $\Delta x = 120$ m.h) reconstructed CFP gather with $\Delta x = 15$ m.

Fig. 4.6 *CFP regularization result using an erroneous operator with a velocity error of 20% in the first layer. Note that the move-out correction is operator-based.*

Contents